

## Unique chemical composition of the very metal-poor star LAMOST J1645+4357\*

WAKO AOKI,<sup>1,2</sup> HAINING LI,<sup>3</sup> NOZOMU TOMINAGA,<sup>1,2,4</sup> TADAFUMI MATSUNO,<sup>5</sup> SATOSHI HONDA,<sup>6</sup> AND GANG ZHAO<sup>3</sup>

<sup>1</sup>*National Astronomical Observatory of Japan, National Institutes of Natural Sciences,  
2-21-1 Osawa, Mitaka, Tokyo 181-8588, Japan*

<sup>2</sup>*Astronomical Science Program, Graduate Institute for Advanced Studies, SOKENDAI, 2-21-1 Osawa, Mitaka, Tokyo 181-8588, Japan*

<sup>3</sup>*Key Lab of Optical Astronomy, National Astronomical Observatories, Chinese Academy of Sciences*

*A20 Datun Road, Chaoyang, Beijing 100012, China*

<sup>4</sup>*Department of Physics, Faculty of Science and Engineering, Konan University, 8-9-1 Okamoto, Kobe, Hyogo 658-8501, Japan*

<sup>5</sup>*Kapteyn Astronomical Institute, University of Groningen  
Landleven 12, 9747 AD Groningen, The Netherlands*

<sup>6</sup>*Nishi-Harima Astronomical Observatory, Center for Astronomy, University of Hyogo  
407-2, Nishigaichi, Sayo-cho, Sayo, Hyogo 679-5313, Japan*

(Received; Revised; Accepted)

Submitted to ApJ

### ABSTRACT

We report on the chemical composition of the very metal-poor ( $[\text{Fe}/\text{H}] = -2.9$ ) star LAMOST J1645+4357 that is identified to be a red giant having peculiar abundance ratios by Li et al. (2022). The standard abundance analysis is carried out for this object and the well studied metal-poor star HD 122563 that has similar atmospheric parameters. LAMOST J1645+4357 has a remarkable abundance set, highlighted by these features: (1) Nitrogen is significantly enhanced ( $[\text{N}/\text{Fe}] = +1.4$ ) and the total abundance of C and N is also very high ( $[(\text{C}+\text{N})/\text{Fe}] = +0.9$ ); (2)  $\alpha$ -elements are over-abundant with respect to iron as generally found in very metal-poor stars; (3) Ti, Sc, Co and Zn are significantly deficient; (4) Cr and Mn are enhanced compared to most of very metal-poor stars; (5) Sr and Ba are deficient and the Sr/Ba ratio ( $[\text{Sr}/\text{Ba}] = -1.0$ ) is significantly lower than the value expected for the r-process. The overall abundance pattern of this object from C to Zn is well reproduced by a faint supernova model assuming spherical explosion, except for the excess of Cr and Mn which requires enhancement of incomplete Si burning or small contributions of a type Ia supernova or a pair-instability supernova. There remains, however, a question why the abundance pattern of this star is so unique among very metal-poor stars.

*Keywords:* stars:abundances — stars:Population II — nuclear reactions, nucleosynthesis, abundances

### 1. INTRODUCTION

The chemical abundance ratios of very metal-poor (VMP) stars hold direct evidence of the yields of first generations of massive stars and supernova explosions (e.g., McWilliam et al. 1995). Extreme examples are carbon-enhanced metal-poor (CEMP) stars with  $[\text{Fe}/\text{H}] < 4$ <sup>1</sup> (Christlieb et al. 2002; Frebel et al. 2005; Keller et al. 2014). The plausible progenitors of these objects are first generations of massive stars ( $10 M_{\odot} < M < 100 M_{\odot}$ ) that have ejected little amount of Fe-peak elements (e.g., Umeda & Nomoto 2003). Another interesting example is the very metal-poor star SDSS J0018–0939 that has low abundances of carbon,  $\alpha$ -elements and elements with odd atomic numbers, which might be produced by explosion of a very massive ( $M > 100 M_{\odot}$ ) star (Aoki et al. 2014). More recently, a clearer chemical signature indicating the existence of very massive stars in the early universe was reported by Xing et al. (2023). The

Corresponding author: Wako Aoki  
aoki.wako@nao.ac.jp

\*

<sup>1</sup>  $[\text{A}/\text{B}] = \log(N_{\text{A}}/N_{\text{B}}) - \log(N_{\text{A}}/N_{\text{B}})_{\odot}$ , and  $\log \epsilon_{\text{A}} = \log(N_{\text{A}}/N_{\text{H}}) + 12$  for elements A and B.

latter examples particularly have a large impact on the estimates of mass distribution of first generation stars that are studied by numerical simulations of star formation from primordial gas clouds.

We conducted high-resolution “snap-shot” spectroscopy with the Subaru Telescope for candidates VMP stars found by the LAMOST survey. The observation obtained medium S/N spectra with short exposures (typically 15-20 minutes) for about 400 stars (Aoki et al. 2022). Abundance results for the whole sample were reported by Li et al. (2022). Among the sample studied by the snap-shot spectroscopy, the extremely metal-poor ( $[\text{Fe}/\text{H}] = -2.9$ ) red giant star LAMOST J164514.95+435712.0 (LAMOST J 1645+4357) shows unusually low abundances of odd elements (Sc and Co) and neutron-capture elements (Sr and Ba). These features are similar to SDSS J0018–0939, although abundances of  $\alpha$ -elements of J1645+4357 are normal. Although carbon is not overabundant, the abundance ratio ( $[\text{C}/\text{Fe}] = 0.33$ ) is higher than those found in typical very metal-poor red giant stars. This star could also be affected by some unusual supernova explosions.

This paper reports on the abundance results for LAMOST J 1645+4357 from follow-up observations to obtain high-resolution blue spectra. The observations and radial velocities obtained from our spectra and by previous work are reported in § 2. The abundance analysis and results for individual elements, as well as comparisons with previous work are presented in § 3. In § 4, we discuss the distinct features of the abundance ratios of LAMOST J 1645+4357 and constraints on properties of the progenitor by comparing the abundance results with supernova models.

## 2. OBSERVATIONS

The first high-resolution spectrum of LAMOST J 1645+4357 was obtained with the Subaru Telescope High Dispersion Spectrograph (HDS; Noguchi et al. (2002)) in observing programs for follow-up spectroscopy of metal-poor star candidates found with LAMOST (Aoki et al. 2022). The snap-shot spectrum with  $R = 36,000$  for 4030–6800 Å was obtained in May 2014 with a short exposure (15 minutes). The abundance result obtained from this snap-shot spectrum was reported by Li et al. (2022). To study more detailed chemical compositions of this star, a high-resolution spectrum of the blue range (3500–5200 Å) with  $R = 60,000$  was obtained with Subaru/HDS on August 30, 2015 with exposure time of 180 minutes.

Standard data reduction procedures were carried out with the IRAF echelle package<sup>2</sup>. The signal-to-noise ratios of the spectrum (per  $1.8 \text{ km s}^{-1}$  pixel) is 120 and 200 at 4000 and 5000 Å, respectively.

The heliocentric radial velocity is measured from isolated spectral lines used for abundance analysis. The result is given in Table 1 with previous measurements with Subaru (Aoki et al. 2022), with Lick/APF by Mardini et al. (2019) and those reported in LAMOST DR5. No significant variation of the radial velocity is found between the two measurements with Subaru, nor in all measurements taking the errors in the LAMOST measurements into consideration. This indicates that there is no signature of binarity for this object from radial velocity measurements to date. We note that LAMOST J 1645+4357 is included in the sample of Price-Whelan et al. (2018) who search for binaries from the APOGEE DR14 data, and is not identified as a “high- $K$  star” (a star likely has a companion).

The atmospheric parameters (effective temperature, surface gravity and metallicity) of LAMOST J1645+4357 are very similar to those of the well-known metal-poor star HD 122563 (Wallerstein et al. 1963; Honda et al. 2006). We select this object as the comparison star for the abundance analysis in the present work. The spectra of HD 122563 obtained with the Subaru/HDS with  $R = 90,000$  (Honda et al. 2004) are adopted for this purpose.

## 3. ABUNDANCE ANALYSIS AND RESULTS

### 3.1. Abundance analysis

We measure equivalent widths by fitting a Gaussian profile. Atomic line data for spectral features are taken from previous studies including Aoki et al. (2013) and those taken from VALD (Kupka et al. 2000). The measured equivalent widths are given in Table 2, together with the line data used in the abundance analysis and sources of the  $gf$  values. We exclude strong absorption lines ( $\log(W/\lambda) > -4.7$ ) from the analysis because they are not sensitive to the elemental abundances due to saturation of absorption. For Na, Al and Si, stronger lines are also used since number of weak absorption lines useful for abundance analysis is not sufficient. Details on the spectral lines for individual elements are reported below.

The solar abundances of Asplund et al. (2009) are adopted to calculate the  $[\text{X}/\text{Fe}]$  values.

<sup>2</sup> IRAF is distributed by the National Optical Astronomy Observatories, which is operated by the Association of Universities for Research in Astronomy, Inc. under cooperative agreement with the National Science Foundation.

We determine the elemental abundances of LAMOST J1645+4357 and HD 122563 by 1D/LTE standard analysis and spectrum synthesis techniques using model atmospheres of the ATLAS NEWODF grid (Castelli & Kurucz (2003)).

The effective temperature of LAMOST J1645+4357 (4660 K) is taken from Li et al. (2022) who determined it from the color  $V - K$ . The surface gravity is derived using the distance information from Gaia EDR3 parallax ( $\log g = 1.01$ ) that is provided by Li et al. (2022). We note that Li et al. (2022) adopted  $\log g$  value derived from spectroscopic analysis with correction ( $\log g = 1.18$ : see Li et al. (2022) for the details) because the Gaia EDR3 data for this object became available after completing their analysis. The metallicity is determined by the Fe abundances from our analysis ( $[\text{Fe}/\text{H}] = -2.86$ ). This result agrees with the Fe abundance ( $[\text{Fe}/\text{H}] = -2.87$ ) determined by Li et al. (2022).

The atmospheric parameters of HD 122563 are adopted from Honda et al. (2006):  $T_{\text{eff}} = 4570$  K,  $\log g = 1.1$ , and  $[\text{Fe}/\text{H}] = -2.77$ . The differences of  $T_{\text{eff}}$ ,  $\log g$ , and  $[\text{Fe}/\text{H}]$  between LAMOST J 1645+4357 and HD 122563 are 90 K, 0.09 dex and 0.09 dex, respectively, demonstrating that HD 122563 is suitable for a reference star.

### 3.2. Abundance results

The carbon and nitrogen abundances are determined by the spectrum synthesis for the CH 4320-4324 Å and CN 3870-3883 Å. The line data are taken from Masseron et al. (2014) and Brooke et al. (2014) for CH and CN, respectively. Figure 1 shows comparisons of spectra between LAMOST J 1645+4357 and HD 122563 in the wavelength ranges covering the CH and CN molecular bands. Both CH and CN bands of LAMOST J 1645+4357 are clearly stronger than those of HD 122563. The nitrogen abundance of LAMOST J 1645+4357 is remarkably high ( $[\text{N}/\text{Fe}] = +1.4$ ). The carbon abundance of this object,  $[\text{C}/\text{Fe}] = +0.3$ , is comparatively high among highly evolved red giants at this metallicity. The carbon to nitrogen ratios of the two objects agree well ( $[\text{C}/\text{N}] = -1.1$ ). This result suggests that LAMOST J 1645+4357 is originally a carbon-enhanced object, but the surface material is already affected by the CN cycle and extra mixing through the evolution in the red giant phase as found in very metal-poor cool red giants including HD 122563 (e.g., Spite et al. 2005).

The wavelength of the [O I] 6300 Å is covered by the snap-shot spectrum. The line, however, overlaps with a telluric absorption line and no useful information on the O abundance is derived from the spectrum.

Abundances of  $\alpha$  and iron-peak elements are determined by the standard analysis of measured equivalent widths. The absorption features of  $\alpha$  elements (Mg, Si and Ca) and Fe of the two objects are very similar, resulting in almost equivalent abundance ratios between the two stars. The comparisons of spectra of the two stars in Figure 2 include Fe lines. Fe lines in LAMOST J 1645+4357 are slightly weaker than those in HD 122563, resulting in lower  $[\text{Fe}/\text{H}]$ . We note that slightly higher temperature of LAMOST J 1645+4357 than that of HD 122563 partially contributes to the weaker Fe lines.

The Na abundances determined from the Na I lines also show good agreement. The Al abundances determined from the Al I 3961 Å are relatively uncertain because the line is severely affected by saturation. The abundance ratios of these two elements ( $[\text{Na}/\text{Fe}]$  and  $[\text{Al}/\text{Fe}]$ ) agree within the errors between the two objects.

Ti I, Ti II and Sc II lines of LAMOST J 1645+4357 are remarkably weaker than those of HD 122563 as found in Figure 2. V II lines detected mostly in the UV range are also weaker in LAMOST J 1645+4357. As a result, the abundance ratios of Sc, Ti and V with respect to Fe of LAMOST J 1645+4357 are significantly lower than those of HD 122563.

On the other hand, the Cr and Mn abundances of LAMOST J 1645+4357 are higher than those of HD 122563. The excess of Cr absorption lines in LAMOST J 1645+4357 compared to HD 122563 is found in Figure 2. The abundance ratios of Cr and Mn ( $[\text{Cr}/\text{Fe}]$  and  $[\text{Mn}/\text{Fe}]$ ) of LAMOST J 1645+4357 are 0.4 dex higher than those of HD 122563.

We note that, since these two elements are underabundant in HD 122563, the abundance ratios of LAMOST J 1645+4357 are just slightly higher than the solar values. Previous studies have reported that Cr abundances derived from Cr I lines are systematically lower than those from Cr II lines for very metal-poor giants (e.g., Honda et al. 2004). The discrepancy is significant in the resonance lines with 0 eV excitation potential ( $\log(W/\lambda) < -4.7$ ). These lines (4254, 4274, and 4289 Å) are not used in the determination of the final Cr abundance because they are stronger than the criterion in our analysis ( $\log(W/\lambda) < -4.7$ ). The abundances derived from the three 0 eV lines are 0.2 dex lower on average than the final abundance, confirming the result obtained by Sneden et al. (2023). Even though these three lines are not included in our study, the Cr abundances determined from this species might be underestimated at very low metallicity because of NLTE effect (Bergemann & Cescutti 2010). Hence, we here just discuss the relative abundance of LAMOST J 1645+4357 with respect to HD 122563.

Among the elements heavier than Fe, Co and Zn are significantly underabundant in LAMOST J 1645+4357 compared to HD 122563, whereas Ni abundances of the two stars agree very well. The Zn abundance of LAMOST J 1645+4357 is determined from the Zn I line at 4722 Å. Another line at 4810 Å that is measured for HD 122563 is not available because the wavelength is affected by the CCD bad column for LAMOST J 1645+4357. The difference of the Zn abundances in these two stars is, however, significant compared to the measurement error.

The Sr abundances are determined from the two resonance lines of Sr II at 4078 and 4215 Å. The [Sr/Fe] of LAMOST J 1645+4357 is remarkably low, whereas that of HD 122563 is high among very metal-poor stars as studied in detail by [Honda et al. \(2006\)](#). We note that the two Sr lines are clearly identified but are not severely saturated in LAMOST J 1645+4357, indicating that the derived abundances are reliable.

The Ba abundances are determined from four Ba II lines for LAMOST J 1645+4357. The effect of hyperfine splitting is included in the calculation using the line data provided by [McWilliam \(1998\)](#) assuming the Ba isotope ratios of the r-process component of solar-system material. The effect is only 0.05 dex for LAMOST J 1645+4357. The effect is larger (0.26 dex) for HD 122563, because the two resonance lines of this object are stronger than those of LAMOST J 1645+4357, and one of the two weaker lines used for LAMOST J 1645+4357 is not available for the analysis of HD 122563. Ba is underabundant in this object as well as in HD 122563.

No other neutron-capture elements than Sr and Ba are detected in the spectrum of LAMOST J 1645+4357. Upper limits of La and Eu abundances are estimated and given in Table 3.

The error of the abundance of each element is also given in the table. The random errors in the measurements ("err" in the table) are estimated to be  $\sigma N^{-1/2}$ , where  $\sigma$  is the standard deviation of derived abundances from individual lines, and  $N$  is the number of lines used. The  $\sigma$  of Fe I ( $\sigma_{\text{FeI}}$ ) is adopted in the estimates for element X for which the number of lines available in the analysis ( $N_X$ ) is small (i.e. the error is  $\sigma_{\text{FeI}} N_X^{-1/2}$ ). Exceptions are Na and Al abundances, which are determined from strong lines. We adopt 0.28 and 0.4 dex for the random errors for these two elements, respectively.

The errors due to the uncertainty of the atmospheric parameters are estimated for a giant, for  $\delta T_{\text{eff}} = 100$  K,  $\delta \log g = 0.3$ , and  $\delta v_{\text{turb}} = 0.3$  km s<sup>-1</sup>. The total errors are given in Table 3. The error is obtained by adding in quadrature the random error and errors due to the uncertainties of stellar parameters.

### 3.3. Comparison with previous work

The abundances of 13 elements of LAMOST J 1645+4357 are reported by [Mardini et al. \(2019\)](#). The effective temperature (4810 K) and  $\log g$  (1.39) adopted in their work based on colors and abundance analysis for Fe I and Fe II lines are slightly higher than our values. The extremely low metallicity ([Fe/H]= -2.97), carbon excess ([C/Fe]= +0.45), low abundances of Sc and Ti ([Sc/Fe]= -0.66, and [Ti/Fe]= -0.10 and -0.21 from Ti I and Ti II) are confirmed by the present work. The very low Ba abundance is also found by [Mardini et al. \(2019\)](#) ([Ba/Fe]= -1.01), although our result is even lower.

The Cr abundance obtained by [Mardini et al. \(2019\)](#) ([Cr/Fe]= -0.43,  $\log \epsilon = 2.24$ ) is lower by 0.55 dex than our result. Four of the six Cr I lines used in their analysis are also measured by our study, but are not adopted to determine the Cr abundance because they are stronger than the criterion adopted in the present work. The four lines include the three resonance lines from which lower Cr abundances are derived (see above). The Cr abundance is determined from nine weaker lines in our analysis. These lines are also applied to the analysis of the comparison star HD 122563, reproducing the Cr abundance obtained by previous studies. Hence, the relatively high Cr abundance of LAMOST J 1645+4357 obtained by the present work is robust.

The low Co abundance determined by the present work ([Co/Fe]= -0.58,  $\log \epsilon = 1.55$ ) is not found by [Mardini et al. \(2019\)](#) ([Co/Fe]= 0.02,  $\log \epsilon = 2.04$ ). Their result is obtained from one line of Co I at 4092 Å. The Co abundance obtained from this line by the present work is  $\log \epsilon = 1.77$ , which is the highest among the abundances from the four lines used in our analysis. Hence, the discrepancy of the Co abundance between the two studies is partially due to the choice of spectral line.

## 4. DISCUSSION AND CONCLUDING REMARKS

Figure 3 exhibits abundance ratios of six elements for LAMOST J 1645+4357 and HD 122563 compared with those of very metal-poor stars studied by [Li et al. \(2022\)](#). Similar figures are presented by [Li et al. \(2022\)](#), but the values for LAMOST J 1645+4357 are updated by the present work. The comparisons of abundance ratios of these elements demonstrate the uniqueness of LAMOST J 1645+4357 among very metal-poor stars.

Figure 4 shows the abundance pattern ( $[X/Fe]$  as a function of atomic number) for LAMOST J 1645+4357 and HD 122563. Figure 5 shows the difference of  $[X/Fe]$  values between the two stars ( $[X/Fe]_{\text{LAMOSTJ1645+4357}} - [X/Fe]_{\text{HD 122563}}$ ).

#### 4.1. Carbon and neutron-capture elements

The luminosity of LAMOST J 1645+4357 ( $\log L = 3.3L_{\odot}$ ) indicates that this object is a highly evolved red giant among extremely metal-poor stars. The C abundance ratios of most of such evolved stars, including HD 122563, are lower than the solar value (i.e.,  $[C/Fe] < 0$ ) as demonstrated by Li et al. (2022). Adopting the criterion of CEMP stars including the effect of internal mixing in red giants, as proposed by Aoki et al. (2007), LAMOST J 1645+4357 is classified into a CEMP star. The large excess of N supports the interpretation that the C abundance ratio is as high as  $[C/Fe] \sim +1$  in the main-sequence phase of this object. Hence, although this star could be nominally classified into a Nitrogen-Enhanced Metal-Poor (NEMP) star, we regard it as a CEMP star. The no excess of Ba indicates that this star is a CEMP-no star. CEMP-no stars with moderate excess of carbon are frequently found in  $[Fe/H] < -2.5$  (Placco et al. 2014).

The very large abundance difference of Sr between the two stars is because of the high Sr abundance of HD 122563 among very metal-poor stars. In addition, LAMOST J 1645+4357 is one of the most Sr deficient objects in very metal-poor stars ( $[Sr/Fe] = -2.4$ ). The Sr/Ba ratio ( $[Sr/Ba] = -1.0$ ) is lower than the value of the r-process component of solar-system material ( $[Sr/Ba] \sim -0.4$ ). Whereas stars with high Sr/Ba ratios are explained by contributions of some process that provides light neutron-capture elements (e.g., LEPP, weak r-process), the low Sr/Ba is expected from the s-process (main s-process) at low metallicity. At the very low metallicity, however, contributions of the main s-process by low-mass or intermediate-mass AGB stars are not expected. Hence, the very low Sr/Ba in this object is a problem to be solved by nucleosynthesis or chemical evolution models for the very early Galaxy. We note that the both Sr and Ba abundances of this object are very low, and, hence, a very small contribution of the s-process could significantly change the Sr/Ba ratio.

Although the origin of neutron-capture elements is unidentified, the low abundances of Sr and Ba suggest that the chemical composition of LAMOST J 1645+4357 is very primitive and would be determined by almost a single event.

#### 4.2. Properties of the progenitor

The high abundance ratios of C and N with respect to Fe in LAMOST J 1645+4357 might be explained by a so-called faint supernova that yields relatively small amount of Fe (Umeda & Nomoto 2003). The models of faint supernovae have been applied to explanations of CEMP-no stars. Panel (a) of Figure 6 shows comparisons of supernova yield models with the abundance ratios of LAMOST J 1645+4357 and HD 122563. The low abundances of Sc, Ti, V, Co and Zn, as well as the overabundances of  $\alpha$ -elements, are naturally explained by a quasi-spherical supernova explosion of  $25 M_{\odot}$  with relatively low explosion energy of  $10^{51}$  ergs and a small amount of Fe ejection of  $0.0078M_{\odot}$ . Explanations of the high abundance ratios of Sc, Ti, V and Co of HD 122563 rather need a high-energy aspherical explosion as proposed for the other EMP stars (e.g., Umeda & Nomoto 2003; Tominaga et al. 2007).

The Cr abundance shown in the figure is the result of the LTE analysis. Taking account of the non-LTE effect, the Cr of HD 122563 would not be underabundant, and that of LAMOST J 1645+4357 would be overabundant. The overabundance of Cr and Mn in LAMOST J 1645+4357 suggests a large contribution of the incomplete Si burning in the explosion. This result might imply that there is some mechanism that enhances the incomplete Si burning layer in the progenitor of LAMOST J 1645+4357. In contrast to the other EMP stars requiring aspherical explosions, the wide incomplete Si burning layer might result from a quasi-spherical explosion with large fallback. Further studies with self-consistent supernova explosion simulations are demanded to investigate the possible connection between incomplete Si burning and sphericity of the explosion.

An alternative possibility is to assume a contribution of another supernova. Panel (b) of Figure 6 shows a comparison of the observed abundance pattern with those obtained by a combination of a faint supernova and a type Ia supernova (CCD2, Iwamoto et al. 1999) that provides Cr and Mn as well as Fe. Here, the faint supernova model ejects a small amount of Fe of  $0.0078M_{\odot}$  and the contribution of type Ia supernova to the total Fe mass in LAMOST J 1645+4357 is 68%. This combination results in a better fit to the observed abundance pattern. A difficulty of this explanation is that a contribution of a type Ia supernova has longer time-scale than core-collapse supernovae and, hence, is not expected to be effective at this very low metallicity. If the timescale of the formation of this object was sufficiently long as a type Ia supernova has contributed, sources of the r-process and the s-process, which might be a merger of

binary neutron stars and AGB stars, respectively, should also be effective. The deficiency of neutron-capture elements of this object, however, does not support contributions of these sources. Furthermore, the relative number fraction of Type Ia SN is 2% that requires a fine tuning.

Another possible scenario is a combination of contributions of a faint supernova and a pair-instability supernova (PISN) with the He core mass of  $100M_{\odot}$  (Heger & Woosley 2002), which provides relatively large amount of iron-peak elements (panel (c) of Figure 6). Here the faint supernova model ejects a small amount of Fe of  $0.0095M_{\odot}$  and the contribution of PISN to the total Fe mass in LAMOST J 1645+4357 is 56%. The relative number fraction of PISN is only 0.2%. The fine tuning is also required to reproduce the abundance pattern. The abundance pattern of elements obtained from this combination, however, does not agree with the observation as in the case of that of a faint supernova and a type Ia supernova, especially the Mn abundance. An advantage of this scenario is that a contribution of a PISN is expected in the very early universe contrary to type Ia supernovae (Salvadori et al. 2019).

In summary, although further investigation is required for understanding the overabundances of Cr and Mn, the overall abundance pattern of LAMOST J 1645+4357 suggests a contribution of a faint supernova with quasi-spherical explosion. A remaining question is why the abundance pattern of this object is so unique among very metal-poor stars: the abundance distributions of very metal-poor stars presented by Li et al. (2022) demonstrates the uniqueness of the abundance ratios of LAMOST J 1645+4357 (Fig. 3). A quasi-spherical explosion of a supernova with low explosion energy is a conventional and natural assumption as a progenitor of very metal-poor stars. The reason why the abundance pattern expected from such an explosion is not observed in other metal-poor stars needs to be explored. The detailed abundance pattern of this star provides a unique opportunity to examine the supernova yields.

#### ACKNOWLEDGMENTS

This research is based on data collected at Subaru Telescope, which is operated by the National Astronomical Observatory of Japan. We are honored and grateful for the opportunity of observing the Universe from Maunakea, which has the cultural, historical and natural significance in Hawaii. Guoshoujing Telescope (the Large Sky Area Multi-Object Fiber Spectroscopic Telescope, LAMOST) is a National Major Scientific Project built by the Chinese Academy of Sciences. Funding for the project has been provided by the National Development and Reform Commission. LAMOST is operated and managed by the National Astronomical Observatories, Chinese Academy of Sciences. This work was supported by JSPS - CAS Joint Research Program. HL and GZ are supported by NSFC No. 11988101. HL is supported by NSFC Nos. 12222305 and 11973049, and the Youth Innovation Promotion Association of the CAS (id. Y202017). WA, NT and SH are supported by JSPS KAKENHI Grant Numbers 21H04499.

*Facilities:* LAMOST, the Subaru Telescope

#### REFERENCES

- Aoki, W., Beers, T. C., Christlieb, N., et al. 2007, ApJ, 655, 492, doi: [10.1086/509817](https://doi.org/10.1086/509817)
- Aoki, W., Tominaga, N., Beers, T. C., Honda, S., & Lee, Y. S. 2014, Science, 345, 912, doi: [10.1126/science.1252633](https://doi.org/10.1126/science.1252633)
- Aoki, W., Beers, T. C., Lee, Y. S., et al. 2013, AJ, 145, 13, doi: [10.1088/0004-6256/145/1/13](https://doi.org/10.1088/0004-6256/145/1/13)
- Aoki, W., Li, H., Matsuno, T., et al. 2022, ApJ, 931, 146, doi: [10.3847/1538-4357/ac6515](https://doi.org/10.3847/1538-4357/ac6515)
- Asplund, M., Grevesse, N., Sauval, A. J., & Scott, P. 2009, ARA&A, 47, 481, doi: [10.1146/annurev.astro.46.060407.145222](https://doi.org/10.1146/annurev.astro.46.060407.145222)
- Bard, A., Kock, A., & Kock, M. 1991, Astron. and Astrophys., 248, 315
- Bard, A., & Kock, M. 1994, Astron. and Astrophys., 282, 1014
- Bergemann, M., & Cescutti, G. 2010, A&A, 522, A9, doi: [10.1051/0004-6361/201014250](https://doi.org/10.1051/0004-6361/201014250)
- Biemont, E., & Godefroid, M. 1980, A&A, 84, 361
- Bizzarri, A., Huber, M. C. E., Noels, A., et al. 1993, A&A, 273, 707
- Blackwell, D. E., Menon, S. L. R., Petford, A. D., & Shallis, M. J. 1982a, MNRAS, 201, 611, doi: [10.1093/mnras/201.3.611](https://doi.org/10.1093/mnras/201.3.611)
- Blackwell, D. E., Petford, A. D., Shallis, M. J., & Leggett, S. 1982b, MNRAS, 199, 21, doi: [10.1093/mnras/199.1.21](https://doi.org/10.1093/mnras/199.1.21)
- Brooke, J. S. A., Ram, R. S., Western, C. M., et al. 2014, ApJS, 210, 23, doi: [10.1088/0067-0049/210/2/23](https://doi.org/10.1088/0067-0049/210/2/23)

- Castelli, F., & Kurucz, R. L. 2003, in *Modelling of Stellar Atmospheres*, ed. N. Piskunov, W. W. Weiss, & D. F. Gray, Vol. 210, A20.  
<https://arxiv.org/abs/astro-ph/0405087>
- Chang, T. N., & Tang, X. 1990, *JQSRT*, 43, 207, doi: [10.1016/0022-4073\(90\)90053-9](https://doi.org/10.1016/0022-4073(90)90053-9)
- Christlieb, N., Bessell, M. S., Beers, T. C., et al. 2002, *Nature*, 419, 904, doi: [10.1038/nature01142](https://doi.org/10.1038/nature01142)
- Davidson, M. D., Snoek, L. C., Volten, H., & Doenszelmann, A. 1992, *A&A*, 255, 457
- Den Hartog, E. A., Lawler, J. E., Sobek, J. S., Sneden, C., & Cowan, J. J. 2011, *ApJS*, 194, 35, doi: [10.1088/0067-0049/194/2/35](https://doi.org/10.1088/0067-0049/194/2/35)
- Frebel, A., Aoki, W., Christlieb, N., et al. 2005, *Nature*, 434, 871, doi: [10.1038/nature03455](https://doi.org/10.1038/nature03455)
- Froese Fischer, C. 1975, *Canadian Journal of Physics*, 53, 184, doi: [10.1139/p75-026](https://doi.org/10.1139/p75-026)
- Fuhr, J. R., Martin, G. A., & Wiese, W. L. 1988, *Journal of Physical and Chemical Reference Data*, Volume 17, Suppl. 4. New York: American Institute of Physics (AIP) and American Chemical Society, 1988, 17
- Garz, T. 1973, *A&A*, 26, 471
- Heger, A., & Woosley, S. E. 2002, *ApJ*, 567, 532, doi: [10.1086/338487](https://doi.org/10.1086/338487)
- Honda, S., Aoki, W., Ishimaru, Y., Wanajo, S., & Ryan, S. G. 2006, *ApJ*, 643, 1180, doi: [10.1086/503195](https://doi.org/10.1086/503195)
- Honda, S., Aoki, W., Kajino, T., et al. 2004, *ApJ*, 607, 474, doi: [10.1086/383406](https://doi.org/10.1086/383406)
- Iwamoto, K., Brachwitz, F., Nomoto, K., et al. 1999, *ApJS*, 125, 439, doi: [10.1086/313278](https://doi.org/10.1086/313278)
- Keller, S. C., Bessell, M. S., Frebel, A., et al. 2014, *Nature*, 506, 463, doi: [10.1038/nature12990](https://doi.org/10.1038/nature12990)
- Kupka, F. G., Ryabchikova, T. A., Piskunov, N. E., Stempels, H. C., & Weiss, W. W. 2000, *Baltic Astronomy*, 9, 590, doi: [10.1515/astro-2000-0420](https://doi.org/10.1515/astro-2000-0420)
- Lawler, J. E., & Dakin, J. T. 1989, *Journal of the Optical Society of America B Optical Physics*, 6, 1457, doi: [10.1364/JOSAB.6.001457](https://doi.org/10.1364/JOSAB.6.001457)
- Lawler, J. E., Guzman, A., Wood, M. P., Sneden, C., & Cowan, J. J. 2013, *ApJS*, 205, 11, doi: [10.1088/0067-0049/205/2/11](https://doi.org/10.1088/0067-0049/205/2/11)
- Lawler, J. E., Sneden, C., & Cowan, J. J. 2015, *ApJS*, 220, 13, doi: [10.1088/0067-0049/220/1/13](https://doi.org/10.1088/0067-0049/220/1/13)
- Li, H., Aoki, W., Matsuno, T., et al. 2022, *ApJ*, 931, 147, doi: [10.3847/1538-4357/ac6514](https://doi.org/10.3847/1538-4357/ac6514)
- Mardini, M. K., Li, H., Placco, V. M., et al. 2019, *ApJ*, 875, 89, doi: [10.3847/1538-4357/ab0fa2](https://doi.org/10.3847/1538-4357/ab0fa2)
- Martin, G. A., Fuhr, J. R., & Wiese, W. L. 1988, *Atomic transition probabilities. Scandium through Manganese*
- Masseron, T., Plez, B., Van Eck, S., et al. 2014, *A&A*, 571, A47, doi: [10.1051/0004-6361/201423956](https://doi.org/10.1051/0004-6361/201423956)
- McWilliam, A. 1998, *AJ*, 115, 1640, doi: [10.1086/300289](https://doi.org/10.1086/300289)
- McWilliam, A., Preston, G. W., Sneden, C., & Searle, L. 1995, *AJ*, 109, 2757, doi: [10.1086/117486](https://doi.org/10.1086/117486)
- Meléndez, J., & Barbuy, B. 2009, *A&A*, 497, 611, doi: [10.1051/0004-6361/200811508](https://doi.org/10.1051/0004-6361/200811508)
- Morton, D. C. 1991, *ApJS*, 77, 119, doi: [10.1086/191601](https://doi.org/10.1086/191601)
- Noguchi, K., Aoki, W., Kawanomoto, S., et al. 2002, *PASJ*, 54, 855, doi: [10.1093/pasj/54.6.855](https://doi.org/10.1093/pasj/54.6.855)
- O'brian, T. R., & Lawler, J. E. 1991, *PhRvA*, 44, 7134, doi: [10.1103/PhysRevA.44.7134](https://doi.org/10.1103/PhysRevA.44.7134)
- O'Brian, T. R., Wickliffe, M. E., Lawler, J. E., Whaling, W., & Brault, J. W. 1991, *Journal of the Optical Society of America B Optical Physics*, 8, 1185
- Pickering, J. C., Thorne, A. P., & Perez, R. 2001, *ApJS*, 132, 403, doi: [10.1086/318958](https://doi.org/10.1086/318958)
- Pinnington, E. H., Berends, R. W., & Lumsden, M. 1995, *Journal of Physics B Atomic Molecular Physics*, 28, 2095, doi: [10.1088/0953-4075/28/11/009](https://doi.org/10.1088/0953-4075/28/11/009)
- Price-Whelan, A. M., Hogg, D. W., Rix, H.-W., et al. 2018, *AJ*, 156, 18, doi: [10.3847/1538-3881/aac387](https://doi.org/10.3847/1538-3881/aac387)
- Ryabchikova, T. A., Hill, G. M., Landstreet, J. D., Piskunov, N., & Sigut, T. A. A. 1994, *MNRAS*, 267, 697, doi: [10.1093/mnras/267.3.697](https://doi.org/10.1093/mnras/267.3.697)
- Salvadori, S., Bonifacio, P., Caffau, E., et al. 2019, *MNRAS*, 487, 4261, doi: [10.1093/mnras/stz1464](https://doi.org/10.1093/mnras/stz1464)
- Smith, G., & O'Neill, J. A. 1975, *Astron. and Astrophys.*, 38, 1
- Smith, G., & Raggett, D. S. J. 1981, *Journal of Physics B Atomic Molecular Physics*, 14, 4015, doi: [10.1088/0022-3700/14/21/016](https://doi.org/10.1088/0022-3700/14/21/016)
- Smith, W. H., & Liszt, H. S. 1971, *Journal of the Optical Society of America (1917-1983)*, 61, 938
- Sneden, C., Boesgaard, A. M., Cowan, J. J., et al. 2023, *arXiv e-prints*, arXiv:2304.06899, doi: [10.48550/arXiv.2304.06899](https://doi.org/10.48550/arXiv.2304.06899)
- Sobek, J. S., Lawler, J. E., & Sneden, C. 2007, *Astrophys. J.*, 667, 1267, doi: [10.1086/519987](https://doi.org/10.1086/519987)
- Spite, M., Cayrel, R., Plez, B., et al. 2005, *A&A*, 430, 655, doi: [10.1051/0004-6361:20041274](https://doi.org/10.1051/0004-6361:20041274)
- Tominaga, N., Umeda, H., & Nomoto, K. 2007, *ApJ*, 660, 516, doi: [10.1086/513063](https://doi.org/10.1086/513063)
- Umeda, H., & Nomoto, K. 2003, *Nature*, 422, 871, doi: [10.1038/nature01571](https://doi.org/10.1038/nature01571)
- Wallerstein, G., Greenstein, J. L., Parker, R., Helfer, H. L., & Aller, L. H. 1963, *ApJ*, 137, 280, doi: [10.1086/147501](https://doi.org/10.1086/147501)
- Wiese, W. L., & Martin, G. A. 1980, *Wavelengths and transition probabilities for atoms and atomic ions: Part 2. Transition probabilities*, Vol. 68

Wood, M. P., Lawler, J. E., Den Hartog, E. A., Sneden, C.,  
& Cowan, J. J. 2014a, ApJS, 214, 18,  
doi: [10.1088/0067-0049/214/2/18](https://doi.org/10.1088/0067-0049/214/2/18)

Wood, M. P., Lawler, J. E., Sneden, C., & Cowan, J. J.  
2013, ApJS, 208, 27, doi: [10.1088/0067-0049/208/2/27](https://doi.org/10.1088/0067-0049/208/2/27)  
— 2014b, ApJS, 211, 20, doi: [10.1088/0067-0049/211/2/20](https://doi.org/10.1088/0067-0049/211/2/20)  
Xing, Q.-F., Zhao, G., Liu, Z.-W., et al. 2023, Nature, 618,  
712, doi: [10.1038/s41586-023-06028-1](https://doi.org/10.1038/s41586-023-06028-1)



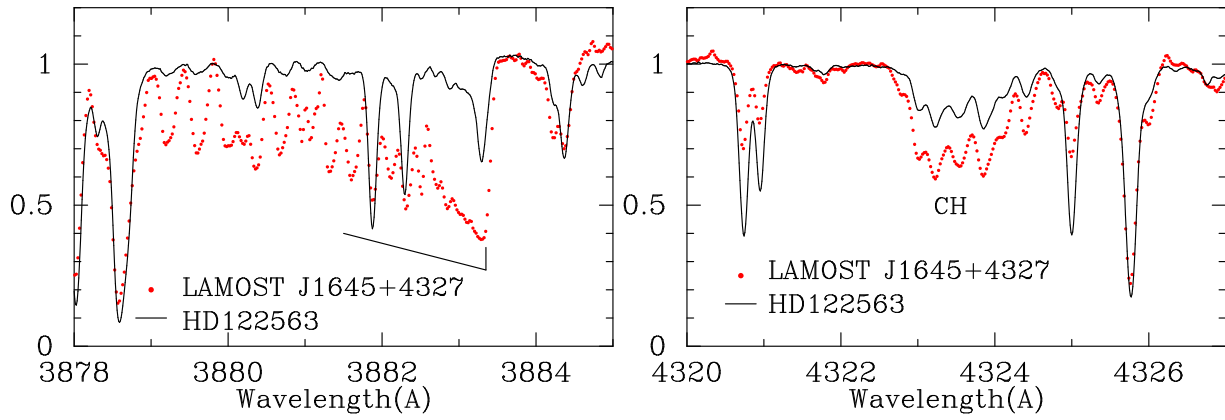


**Figure 1.** Comparison of spectra of LAMOST J1645+4327 (red filled circles) and HD 122563 (line) for the wavelength ranges including CH and CN molecular bands.

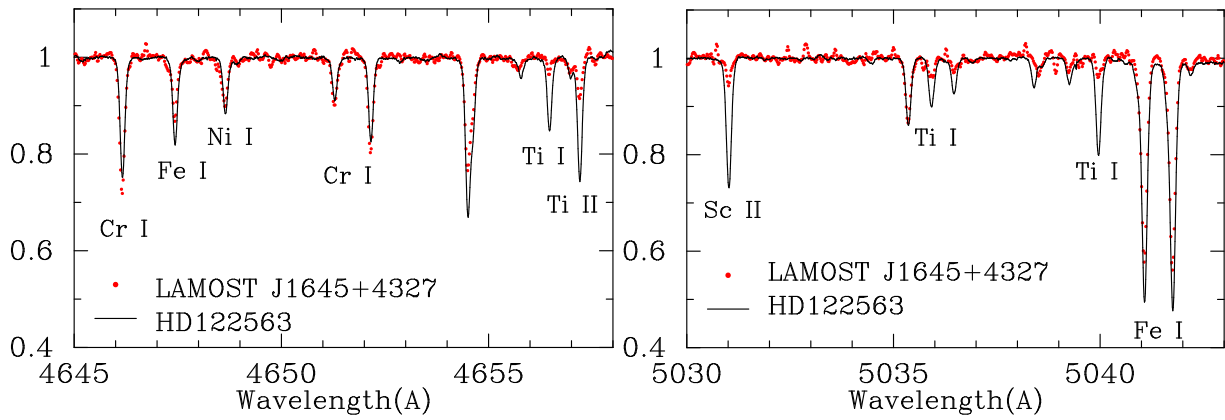


**Figure 2.** Comparison of spectra of LAMOST J1645+4327 (red filled circles) and HD 122563 (line).

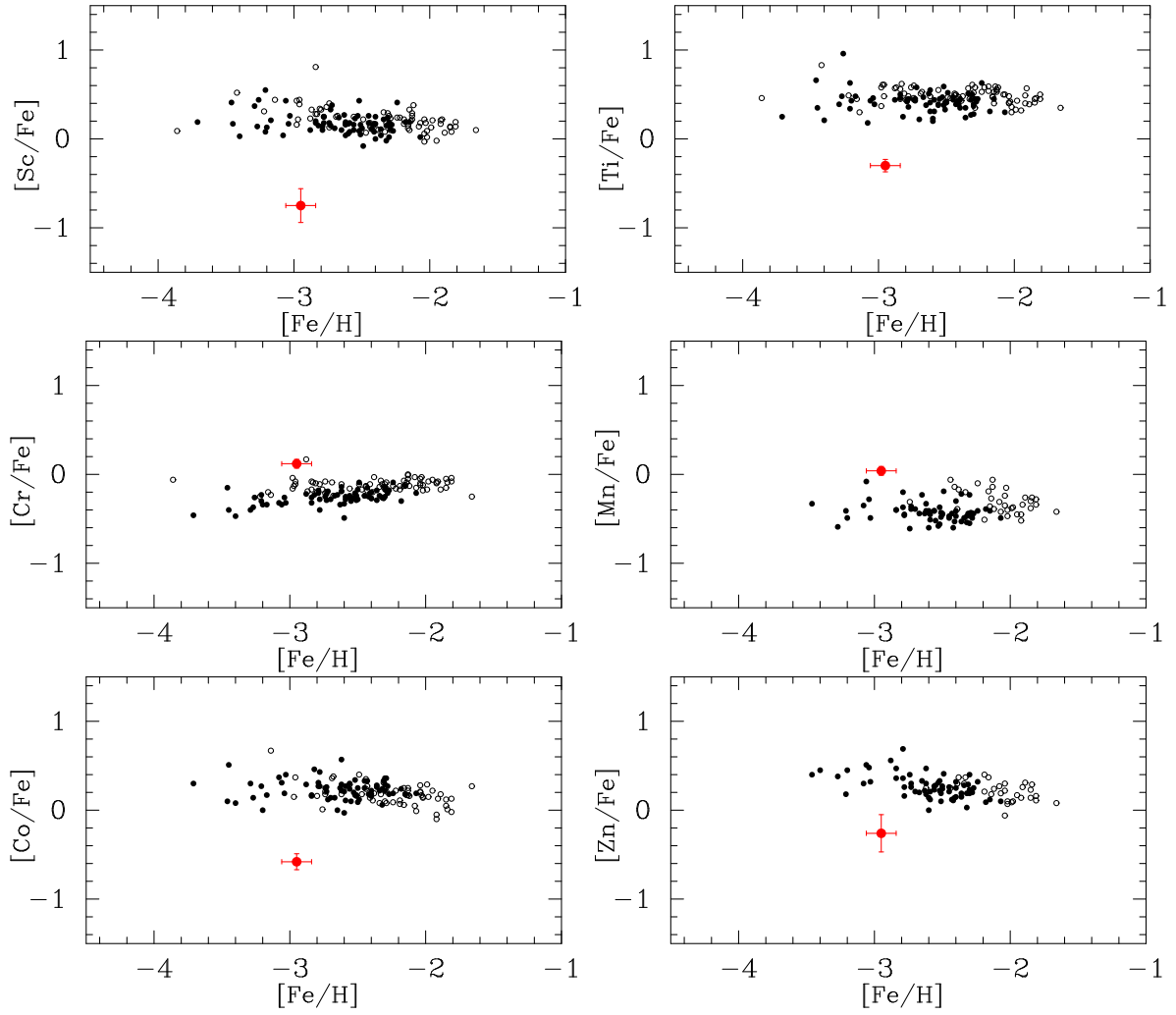


**Figure 3.** Abundance ratios of LAMOST J 1645+4357 (red filled circle with error bars) and very metal-poor stars studied by Li et al. (2022) (filled circles for stars with  $T_{\text{eff}} < 5500$  K and open circles for stars with  $T_{\text{eff}} \geq 5500$  K). For the sample of Li et al. (2022), stars for which abundances were determined from spectra with signal-to-noise ratios higher than 50 are presented.

0

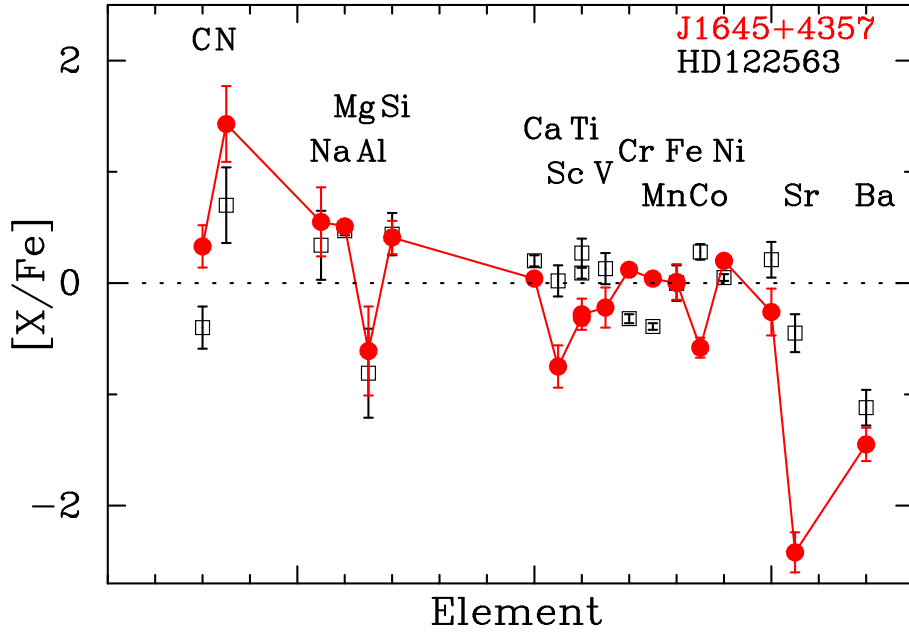


**Figure 4.** The abundance patterns ( $[X/Fe]$ ) of LAMOST J1645+4357 (filled circles with line) and HD 122563 (open squares). The error bars indicate the errors of  $[X/Fe]$  including the uncertainties of atmospheric parameters.

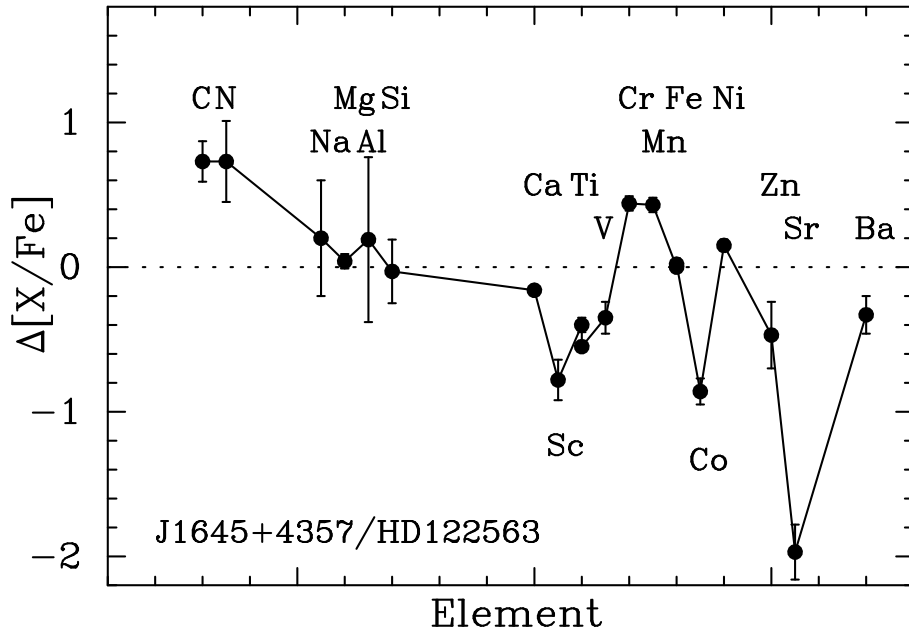


**Figure 5.** The difference of  $[X/Fe]$  values between the two stars ( $[X/Fe]_{\text{LAMOST J1645+4357}} - [X/Fe]_{\text{HD 122563}}$ ). The error bars indicate the root sum of the squares of random errors estimated for the two objects.

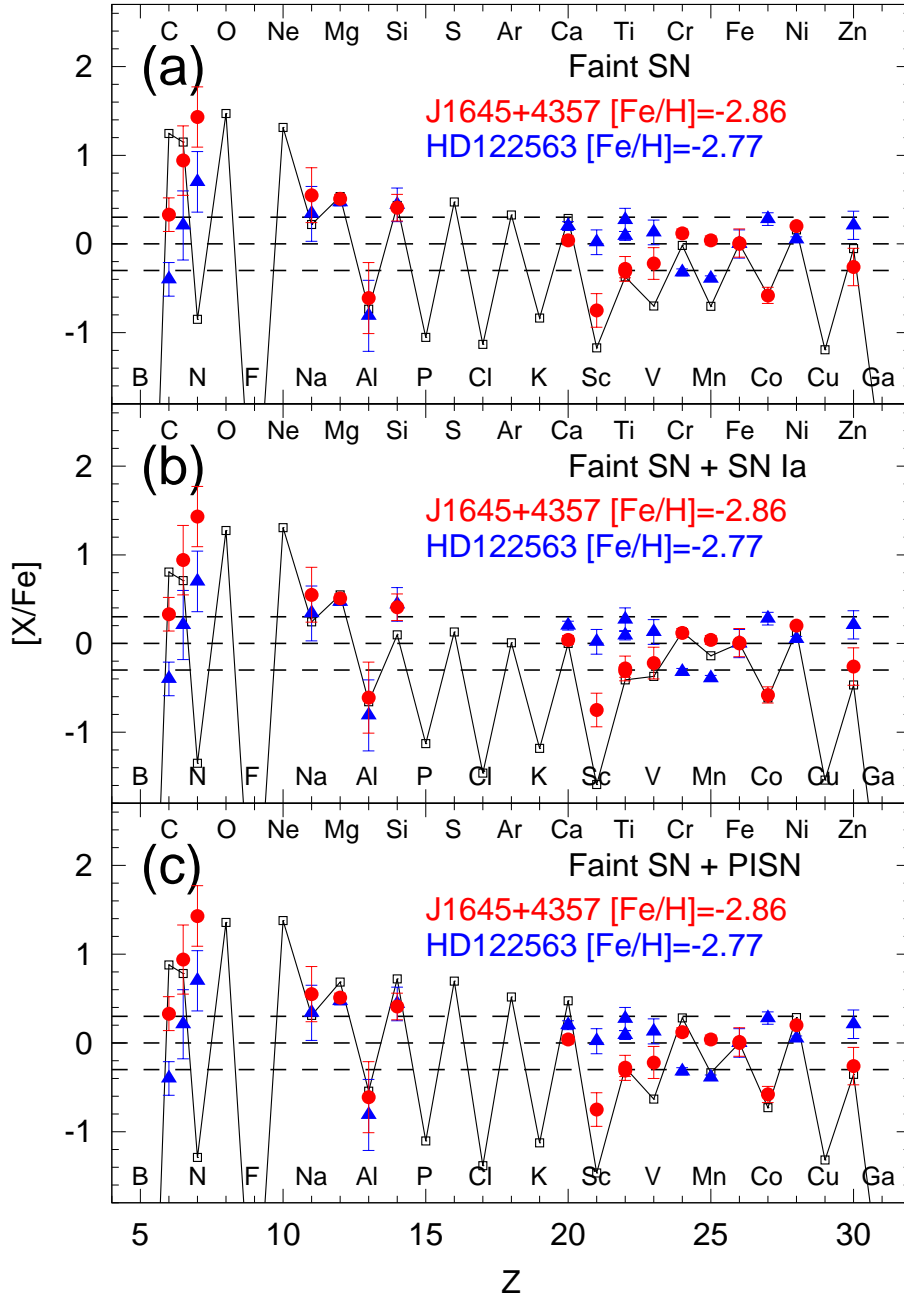


**Figure 6.** Elemental abundance ratios of LAMOST J 1645+4357 and HD 122563 compared with models for (a) a faint SN, (b) a faint SN and a Type Ia SN, and (c) a faint SN and a PISN.

**Table 1.** Radial velocities

Obs. date	MJD	$V_{\text{Helio}}$	Telescope (ref.)
May 6, 2013	56418	-90.4	LAMOST (DR5)
May 11, 2013	56423	-84.9	LAMOST (DR5)
April 14, 2017	57857	-79.0	LAMOST (DR5)
May 28, 2015	57170	-83.20	Lick/APF (Mardini et al. 2019)
May 10, 2014	56787	-84.4±0.3	Subaru (Aoki et al. 2022)
August 30, 2015	57264	-84.6±0.3	Subaru (This work)

**Table 2.** Spectral line data and equivalent widths

Species	Wavelength (Å)	$\chi$ (eV)	$\log gf$	$W$ (mÅ)	References
Na I	5889.951	0.101	0.000	194.4	1
Na I	5895.924	-0.197	0.000	166.7	1
Mg I	4167.271	-0.710	4.346	48.5	2
Mg I	4571.096	-5.688	0.000	75.0	1

References – (1)Morton (1991); (2)Froese Fischer (1975); (3)Chang & Tang (1990); (4)Smith & Liszt (1971); (5)O’brian & Lawler (1991); (6)Garz (1973); (7)Wiese & Martin (1980); (8)Smith & O’Neill (1975); (9)Smith & Raggett (1981); (10)Lawler et al. (2013); (11)Blackwell et al. (1982a); (12)Blackwell et al. (1982b); (13)Sobeck et al. (2007); (14)Martin et al. (1988); (15)Den Hartog et al. (2011); (16)O’Brian et al. (1991); (17)Fuhr et al. (1988); (18)Bard & Kock (1994); (19)Bard et al. (1991); (20)Lawler et al. (2015); (21)Wood et al. (2014b); (22)Biemont & Godefroid (1980); (23)Lawler & Dakin (1989); (24)Wood et al. (2013); (25)Bizzarri et al. (1993); (26)Ryabchikova et al. (1994); (27)Pickering et al. (2001); (28)Wood et al. (2014a); (29)Meléndez & Barbuy (2009); (30)Pinnington et al. (1995); (31)McWilliam (1998); (32)Davidson et al. (1992). (This table is available in its entirety in machine-readable form.)

**Table 3.** Abundance results

Element	Sun	HD122563					J1645+4357					$\Delta$ J1645/HD122563	
	$\log \epsilon(X)$	$\log \epsilon(X)$	[X/Fe]	$N$	err	$\text{err}_{\text{tot}}^a$	$\log \epsilon(X)$	[X/Fe]	$N$	err	$\text{err}_{\text{tot}}^a$	$\Delta_{\text{J1645/HD122563}}$	$\text{err}_{\Delta}^b$
C	8.43	5.30	-0.40		0.10	0.19	5.90	0.33		0.10	0.19	0.73	0.14
N	7.83	5.80	0.70		0.20	0.34	6.40	1.43		0.20	0.34	0.73	0.28
Na	6.24	3.85	0.34	2	0.28	0.31	3.93	0.55	2	0.28	0.31	0.20	0.40
Mg	7.60	5.34	0.47	4	0.02	0.04	5.25	0.51	4	0.04	0.05	0.04	0.05
Al	6.45	2.91	-0.81	1	0.40	0.40	2.98	-0.61	1	0.40	0.40	0.19	0.57
Si	7.51	5.22	0.44	1	0.18	0.19	5.07	0.41	2	0.14	0.15	-0.03	0.22
Ca	6.34	3.81	0.20	12	0.02	0.05	3.52	0.04	13	0.03	0.05	-0.16	0.03
Sc	3.15	0.44	0.02	4	0.04	0.14	-0.46	-0.75	2	0.14	0.19	-0.78	0.14
Ti I	4.95	2.31	0.09	30	0.02	0.05	1.78	-0.31	17	0.05	0.07	-0.40	0.05
Ti II	4.95	2.49	0.27	29	0.02	0.13	1.82	-0.28	21	0.02	0.14	-0.55	0.03
V	3.93	1.32	0.13	5	0.03	0.14	0.85	-0.22	3	0.11	0.18	-0.35	0.11
Cr	5.64	2.59	-0.32	9	0.02	0.04	2.90	0.12	9	0.05	0.05	0.44	0.05
Mn	5.43	2.30	-0.39	5	0.02	0.03	2.61	0.04	4	0.04	0.05	0.43	0.05
Fe I	7.50	4.77	0.00	137	0.02	0.02	4.64	0.00	144	0.02	0.02	0.00	0.03
Fe II	7.50	4.76	0.00	12	0.02	0.16	4.66	0.01	12	0.03	0.16	0.02	0.04
Co	4.99	2.54	0.28	7	0.05	0.07	1.55	-0.58	4	0.07	0.09	-0.86	0.09
Ni	6.22	3.54	0.05	6	0.03	0.03	3.56	0.20	4	0.02	0.02	0.15	0.04
Zn	4.56	2.04	0.21	2	0.13	0.16	1.44	-0.26	1	0.19	0.21	-0.47	0.23
Sr	2.87	-0.32	-0.45	2	0.13	0.17	-2.41	-2.42	2	0.14	0.18	-1.97	0.19
Ba	2.18	-1.67	-1.12	3	0.10	0.16	-2.13	-1.45	4	0.08	0.15	-0.33	0.13
La	1.10	-2.50	-0.87				< -2.50	< -0.74					
Eu	0.52	-2.85	-0.64	3			< -3.20	< -0.86					

<sup>a</sup>Errors of [X/Fe] values including random errors and errors due to uncertainties of atmospheric parameters.

<sup>b</sup>Errors obtained by adding in quadrature the random errors of the two stars.